

***LANDYNE***

# **User Manual**

**Simulation and Analysis of Kikuchi Patterns**

**+ SAED Patterns Including Double Diffraction Effect**

Copyright 2011-2024 LANDYNE ©

All Right Reserved

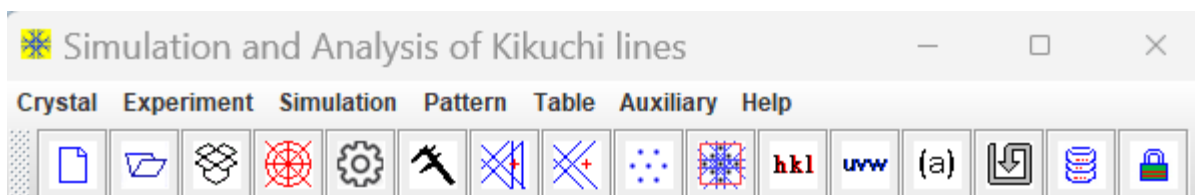


## Table of Contents

<b>Highlight .....</b>	<b>3</b>
<b>1. Introduction.....</b>	<b>3</b>
<b>2. Theory background .....</b>	<b>4</b>
2.1 <i>Simulation of Kikuchi pattern .....</i>	5
2.2 <i>The determination of the precise orientation from three Kikuchi bands .....</i>	5
2.3 <i>The determination of the precise orientation from two Kikuchi bands .....</i>	7
2.4 <i>Kikuchi map .....</i>	9
2.5 <i>Double diffraction effect .....</i>	10
<b>3. The graphic user interface of SAKI .....</b>	<b>11</b>
3.1 <i>Main interface.....</i>	11
3.2 <i>Tools and options.....</i>	11
<b>4. Usage of SAKI .....</b>	<b>11</b>
4.1 <i>Prepare new data file.....</i>	12
4.2 <i>Simulation .....</i>	12
4.3 <i>Sava figures for publication.....</i>	14
4.4 <i>Load an experimental image.....</i>	14
4.5 <i>Operation steps for analysis .....</i>	14
<b>5. Application examples.....</b>	<b>16</b>
5.1 <i>Simulation of spot and Kikuchi diffraction patterns .....</i>	16
5.2 <i>Precise orientation determination from three Kikuchi bands.....</i>	17
5.3 <i>Precise orientation determination from two Kikuchi bands.....</i>	19
<b>6. Related components in Landyne suite .....</b>	<b>20</b>
6.1 <i>SVAT software.....</i>	20
6.2 <i>SAED software.....</i>	20
6.3 <i>SPICA software.....</i>	20
<b>References .....</b>	<b>21</b>

## Highlight

- Use a provided template for creating new crystal structures.
- Employ SAKI for simulating Kikuchi lines and SAED patterns with a double diffraction effect.
- Utilize a user-friendly index system for Kikuchi lines and SAED patterns.
- Convert between Miller and Miller-Bravais indices.
- Perform drag-and-drop actions to load experimental diffraction patterns (.jpg, .png and .tif).
- Align, resize, rotate, and invert experimental SAED/Kikuchi patterns.
- Compare experimental SAED patterns with three Kikuchi pairs (three Kikuchi poles) or two Kikuchi pairs (single Kikuchi pole) to determine precise crystal phase orientation.
- Analyze experimental SAED patterns to detect forbidden diffraction due to the double diffraction effect.
- Save SAED patterns with Kikuchi lines in .tif, .jpg, .png, and .gif formats.
- Create labeled figures suitable for publication.
- Access a periodic table of elements with a molecular mass calculator.
- Access a table listing the number and symbols of the 230 space groups.

## 1. Introduction

Selected area electron diffraction (SAED) analysis has been extensively used in materials science for phase identification, interpretation of twins, coexisting multiple phases, and so forth. The simulation of electron diffraction patterns plays a vital role in interpreting experimental results.

The selected-area mode in a transmission electron microscope can produce three types of electron diffraction patterns, as shown in Table 1.

Table 1. Diffraction patterns in a transmission electron microscope with a parallel incident beam.

	<b>Diffraction pattern</b>	<b>TEM Specimen</b>	<b>Landyne software</b>
(a)	Ring pattern	Polycrystalline specimen	PCED and QPCED
(b)	Spot pattern	Single-crystal region of the specimen	SAED and QSAED
(c)	Kikuchi line pattern		SAKI and SPICA

Diffraction patterns in cases (b) and (c) often occur on the same diffraction pattern. Kikuchi patterns consist of pairs of parallel bright and dark lines. Kikuchi patterns are taken from a single-crystal region of the specimen, which is reasonably thick (~1/2 maximum usable penetration) and has a low defect density.

Kikuchi patterns are significant for the following reasons [Edington, 1975],

- (i) They enable the tasks of obtaining a zone axis of diffraction pattern to be performed more accurately than with spot patterns.

- (ii) They constitute a “Kikuchi map,” which describes the distribution of Kikuchi lines within a unit triangle of the stereogram, which can be simulated with Landyne SPICA. The specimen may be tilted in a self-consistent manner while working in the microscope.
- (iii) They determine the sign and magnitude of the deviation  $s_g$  from the exact Bragg position. The relationship between the bright Kikuchi line and its associated diffraction spot is used.
- (iv) They define the sense of tilt because the Kikuchi pattern behaves as if it is fixed to the crystal’s bottom. Consequently, it moves in the same sense as the crystal; that is, the lines move in a direction perpendicular to the tilt axis and towards the edge of the specimen tilted up.
- (v) Small angular tilts,  $\delta$ , can be estimated, where  $\delta = m/L$  and  $m$  is the linear displacement of the Kikuchi line pattern, normal to the tilt axis;  $L$  is the camera length.
- (vi) Large angular tilts can be measured by identifying specific  $\mathbf{B} = \mathbf{g}_1 \wedge \mathbf{g}_2$  accurately.
- (vii) They determine crystal symmetry because, unlike spot patterns, Kikuchi patterns exhibit real crystal symmetry.

SAKI, currently in version 6, is specifically designed for simulating and analyzing Kikuchi patterns with Selected Area Electron Diffraction (SAED), incorporating a double diffraction effect. It serves as a pivotal component within the Landyne suite, dedicated to electron diffraction simulation and crystallographic analysis.

## 2. Theory background

When a transmission electron microscopy (TEM) sample is sufficiently thick to remain electron-transparent, incoherent scattering contributes a diffuse background to its diffraction pattern. Overlaying this background are intersecting sets of straight lines known as Kikuchi lines. These lines, whether bright or dark, exhibit remarkable straightness and regular arrangement, providing crucial crystallographic information about the sample.

In CBED (Convergent Beam Electron Diffraction) patterns, Kikuchi lines tend to be more pronounced compared to SAED (Selected Area Electron Diffraction) patterns due to two primary reasons: i) CBED patterns originate from a smaller and more uniform region, and ii) there is an amplification of coherent and elastic scattering in CBED.

The fundamental geometric features of Kikuchi patterns can be comprehended using a simplified approach first proposed by Kikuchi in 1928. According to this model, the lines result from the diffraction of electrons that have undergone prior inelastic scattering within the specimen. In SAED patterns, these inelastically scattered electrons appear as a diffuse halo surrounding the transmitted and strongly diffracted spots, contributing to overall faint background intensities. As the distance from the transmitted beam increases, the diffuse halo diminishes in intensity due to the prevalence of smaller energy changes among scattered electrons. This intensity distribution can be effectively described using a polar diagram, as depicted in Figure 1.

### 2.1 Simulation of Kikuchi pattern

Kikuchi lines are useful for the precise determination of the specimen orientation in TEM experiments. The location of the Kikuchi line is related to the sign and magnitude of the deviation parameter,  $s_g$  of the diffraction spot with a vector of  $g$ ,

$$x = \frac{sR}{g^2 \lambda}$$

where  $x$  is the distance from the diffraction spot at  $R$  to its corresponding bright Kikuchi line;  $\lambda$  is the incident electron beam's wavelength.

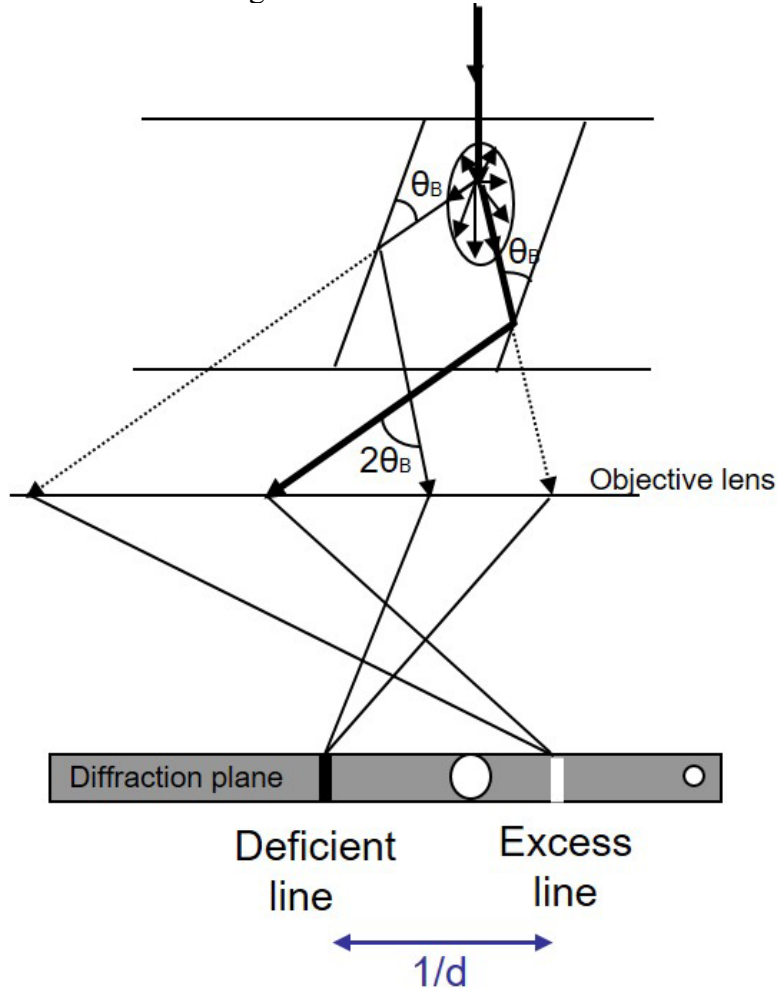


Figure 1. The geometry of Kikuchi lines in electron diffraction of a single crystal.

### 2.2 The determination of the precise orientation from three Kikuchi bands

The analysis for the crystal orientation unambiguously requires three nonparallel Kikuchi line pairs in a SAED pattern. The direction of the incident electron beam ( $OO'$ ) is specified in the angles to the zone axes of the Kikuchi poles (A, B, and C) in Figure 2,

$$\phi \approx R/L$$

Where  $R$  is the distance of  $OA$ ,  $OB$ , and  $OC$ , while  $L$  is the camera length.

Due to the inward curvature of the Ewald sphere, indices, and zone axes satisfy,

$$(hkl) * [uvw] > 0$$

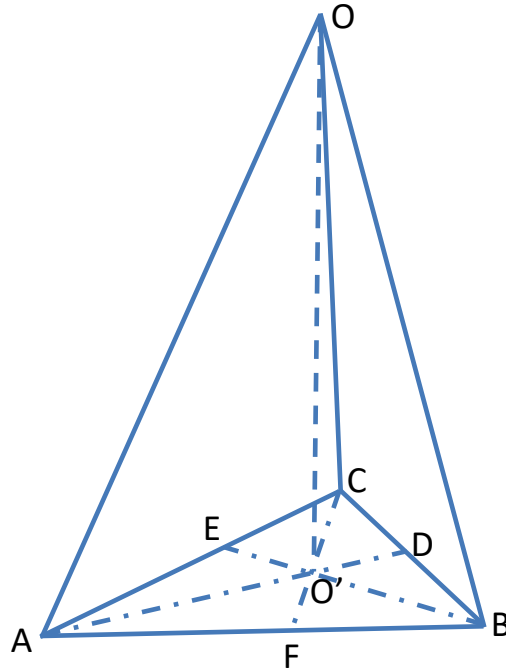


Figure 2. The incident beam (OO') and Kikuchi poles (OA, OB, OC) are related.

Here, the (h k l) refers to the outer line of each Kikuchi pair, and the [u v w] refers to the other Kikuchi pole, which is on the side of the Kikuchi pair. SAKI provides a step-by-step approach to analyze the precise orientation from a set of three Kikuchi line pairs in a SAED pattern.

The precise orientation of the crystal can be derived from the incident electron beam positions and three Kikuchi poles. SAKI analysis can be applied to all seven crystal systems.

Method 1. Analytical equations

$$\cos(\Phi_i) = \frac{\mathbf{u}_i \cdot \mathbf{r}}{|\mathbf{u}_i| |\mathbf{r}|}$$

Let's assume  $|\mathbf{r}| = 1$ , three linear equations can be solved,  $\mathbf{r} = [u, v, w]$ .

Method 2. Vector analysis

$$f_1 = \frac{1}{\cos\phi_1} = \sqrt{1 + \left(\frac{AO'}{OO'}\right)^2}$$

$$f_2 = \frac{1}{\cos\phi_2} = \sqrt{1 + \left(\frac{BO'}{OO'}\right)^2}$$

$$f_3 = \frac{1}{\cos\varphi_3} = \sqrt{1 + \left(\frac{CO'}{OO'}\right)^2}$$

$$\overrightarrow{OA} = f_1 \frac{OO'}{|u_1 v_1 w_1|} [u_1 v_1 w_1]$$

$$\overrightarrow{OB} = f_2 \frac{OO'}{|u_2 v_2 w_2|} [u_2 v_2 w_2]$$

$$\overrightarrow{OC} = f_3 \frac{OO'}{|u_3 v_3 w_3|} [u_3 v_3 w_3]$$

$$[uvw] = \overrightarrow{OO'} = \frac{O'D}{AD} \overrightarrow{OA} + \frac{O'E}{BE} \overrightarrow{OB} + \frac{O'F}{CF} \overrightarrow{OC}$$

We notice the relation,

$$1 = \frac{O'D}{AD} + \frac{O'E}{BE} + \frac{O'F}{CF} .$$

### 2.3 The determination of the precise orientation from two Kikuchi bands

Here, we adopted the ODS method by Otte, Dash and Schaak (1964) and the HF-K method by Helfmeier and Feller-Kniepmeer (1977) for the orientation along the primary beam from two independent Kikuchi pairs (or a single Kikuchi pole).

In the two methods, it is assumed that the Kikuchi pairs were indexed, and the positions of the incident beam and the Kikuchi pairs were located.

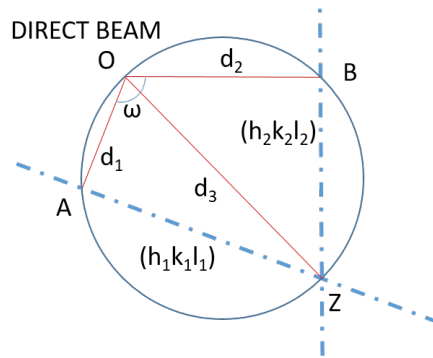


Figure 3. The traces of the diffracting planes,  $(h_1k_1l_1)$  and  $(h_2k_2l_2)$ . The symbols used in describing the orientation determination from the Kikuchi pattern.

We introduced the ODS method first. As shown in Figure 3, two traces, AZ and BZ, from planes (h1k1l1) and (h2k2l2), respectively, are drawn intersecting at Z, which is the zone axis. Now, the points OAZB lie in a circle, so it follows that

$$OI = d_3 = (d_1^2 + d_2^2 - 2d_1d_2\cos\omega)^{1/2}/\sin\omega \quad (1)$$

where  $d_1$ ,  $d_2$ , and  $\omega$  are the distances OA, OB, and the angle  $\angle AOB$ , respectively. The diagram has been redrawn and relabeled to make the two methods easier to compare. A typo in the formula [1] in the original paper has been corrected.

If the effective camera length is  $L$ , the distances  $d_1$ ,  $d_2$ , and  $d_3$  correspond to the small angles (less than  $5^\circ$  in general, since  $L \gg d$ )  $\sin\chi_1 \approx \chi_1 = d_1/L$ ,  $\sin\chi_2 \approx \chi_2 = d_2/L$ ,  $\sin\chi_3 \approx \chi_3 = d_3/L$ . Respectively, these are the angles between the directions OA and  $\hat{\mathbf{p}} = [h_1k_1l_1]$ , OB and  $\hat{\mathbf{q}} = [h_2k_2l_2]$ ,  $\hat{\mathbf{k}}$  and  $\pm(\hat{\mathbf{p}} \times \hat{\mathbf{q}}) \parallel \hat{\mathbf{r}} = [h_3k_3l_3]$  where  $\hat{\mathbf{k}}$  is the normal to the plane of the diffraction pattern.  $\hat{\mathbf{p}}$ ,  $\hat{\mathbf{q}}$ ,  $\hat{\mathbf{r}}$  and  $\hat{\mathbf{k}}$  are all unit vectors.

We have that

$$\hat{\mathbf{k}} = e_1\hat{\mathbf{p}} + e_2\hat{\mathbf{q}} + e_3\hat{\mathbf{r}} \quad (2)$$

where

$$e_1 = \frac{\sin\chi_1 - \sin\chi_2\cos\delta}{\sin^2\delta}, \quad (3)$$

$$e_2 = \frac{\sin\chi_2 - \sin\chi_1\cos\delta}{\sin^2\delta}, \quad (4)$$

$$e_3 = (\sin^2\delta - \sin^2\chi_1 - \sin^2\chi_2 + 2\cos\delta\sin\chi_1\sin\chi_2)^{1/2}/\sin\delta, \quad (5)$$

$$\cos\delta = \hat{\mathbf{p}} \cdot \hat{\mathbf{q}}, \quad \sin\delta = |\hat{\mathbf{p}} \times \hat{\mathbf{q}}| \quad (6)$$

The HF-K method: The solution is derived from a tripod of  $\mathbf{g}_1$ ,  $\mathbf{g}_2$ , and  $\mathbf{Z} = \mathbf{g}_1 \times \mathbf{g}_2$ . To compare the ODS method, we reassign  $\hat{\mathbf{p}} = \frac{\mathbf{g}_1}{|\mathbf{g}_1|}$ ,  $\hat{\mathbf{q}} = \frac{\mathbf{g}_2}{|\mathbf{g}_2|}$  and  $\hat{\mathbf{r}} = \frac{\mathbf{Z}}{|\mathbf{Z}|}$ . The proper negative beam direction  $\hat{\mathbf{k}}$  is therefore given by

$$\hat{\mathbf{k}} = \hat{\mathbf{r}} - L_1f_1\hat{\mathbf{p}} - L_2f_2\hat{\mathbf{q}} \quad (7)$$

where  $L_1$  and  $L_2$  are the sides of the parallelogram in Fig. 4, and the  $f_i$  ( $i = 1, 2$ ) is the factor converting measured distances into angles. The diagram has been redrawn and relabeled to make the two methods easier to compare. The only data to be measured from the pattern are the spacings of the two Kikuchi pairs,  $b_1$  and  $b_2$ , and the angle ( $\omega$ ) between them. The analytical solutions for  $L_1$  and  $L_2$  are

$$L_1 = \frac{d_1 - d_2\cos\omega}{\sin^2\omega} \quad (8)$$

$$L_2 = \frac{d_2 - d_1\cos\omega}{\sin^2\omega} \quad (9)$$

The conversion factor can be calculated to be

$$f_i = \tan\left[2\arcsin\left(\frac{g_i}{2k}\right)\right]/b_i, \quad (10)$$

Here  $g_i$  is the length of a reciprocal lattice vector,  $k$  equals  $1/\lambda$ , and  $\lambda$  is the wavelength.

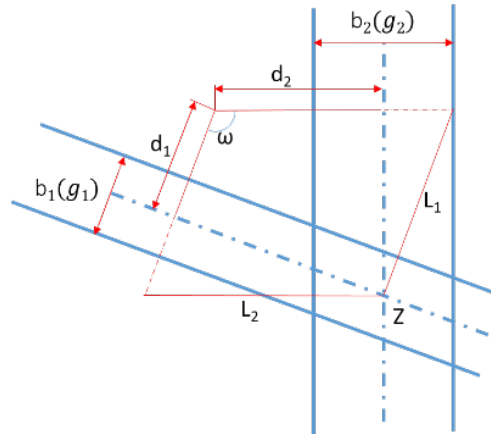


Figure 4. Schematic diagram demonstrating analysis of Kikuchi line pairs.

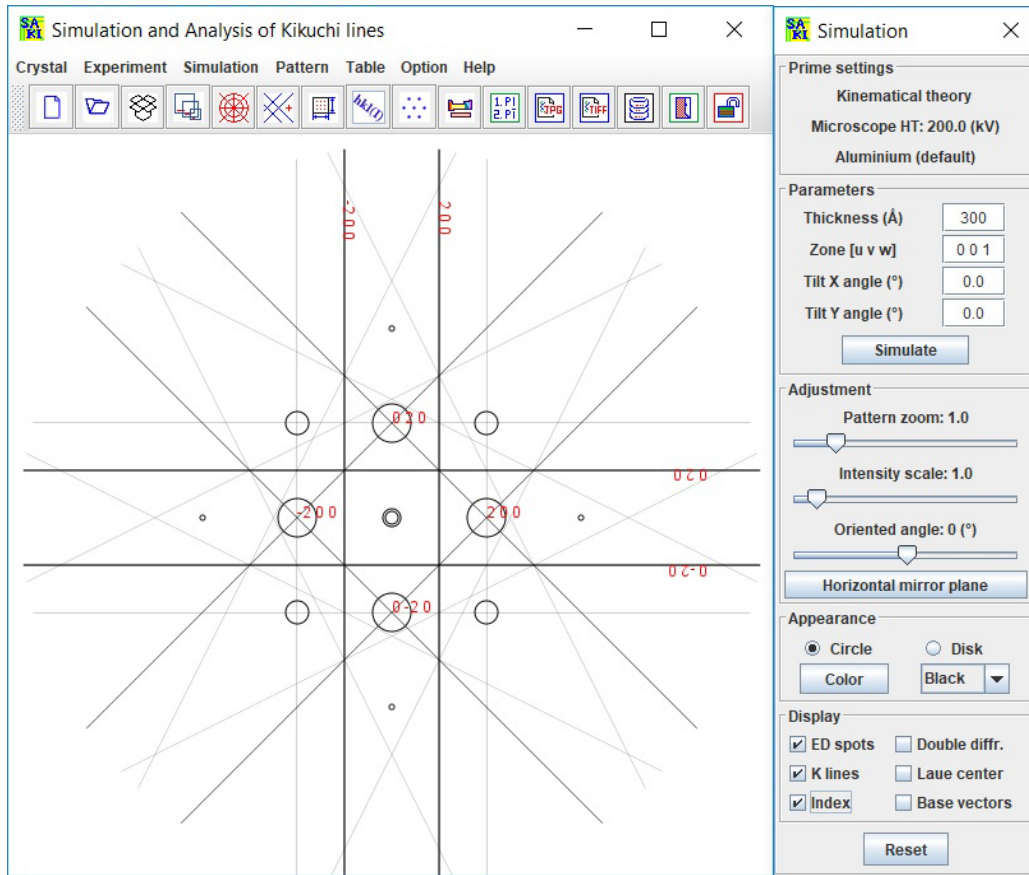


Figure 5. A snapshot of the main panels in SAKI with a simulated Kikuchi pattern of Al [001].

## 2.4 Kikuchi map

Kikuchi maps consist of a montage of Kikuchi patterns taken with different incident electron beams positioned in the stereogram's unit triangle's corresponding place. All the Kikuchi lines join up to produce a 'road' map of the unit triangle. The simulation of Kikuchi is given in SPICA software.

### 2.5 Double diffraction effect

When a TEM specimen is thin enough, only single scattering events need to be considered to interpret the experimental results. Otherwise, multiple beam dynamical scattering must be used for analysis. Double diffraction is a simplified model where an electron diffracts twice before leaving the specimen, requiring the electron beam from the first diffraction to serve as the incident beam for the second diffraction. Most TEM samples are sufficiently thick that electrons can undergo multiple diffractions, especially when  $s \approx 0$ . Detailed calculations using dynamical theory become unavoidable in such cases. However, some aspects of multiple diffractions can be understood through straightforward geometrical considerations and kinematical theory. For example, the occurrence of forbidden diffraction spots and interactions between two crystallites can be explained this way. SAKI deals with the first case, where the central idea is that a diffracted electron acts as an incident beam for the second diffraction.

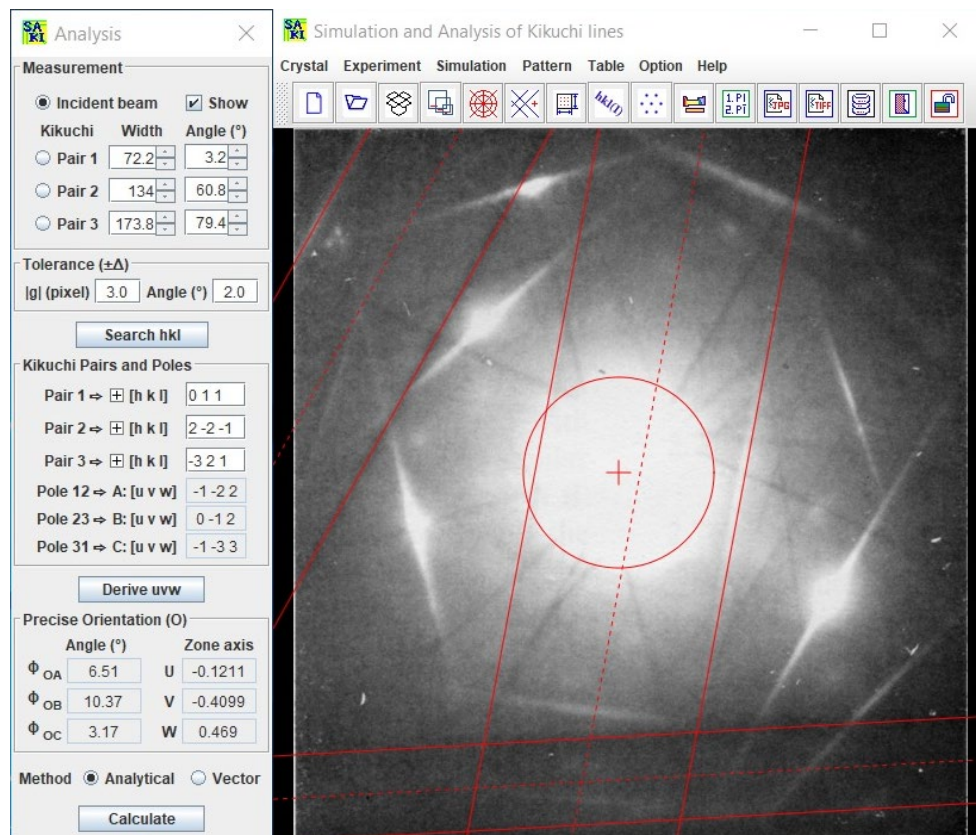


Figure 6. A snapshot of the main panels in SAKI, including a Kikuchi pattern of Mg.

### 3. The graphic user interface of SAKI

#### 3.1 Main interface

The main interface of SAKI features a frame with a menu, a toolbar, and a calculation dialogue panel, as illustrated in Figure 5. Figure 6 shows the SAKI frame with an experimental SAED pattern and an analysis dialogue panel. The menu provides detailed text descriptions organized into groups, while the toolbar offers graphical icons for easy access. Most functions available in the menu are also accessible via the toolbar, though some functions are exclusive to the toolbar. Users can adjust the size of the frame and the display panel according to their preferences.

#### 3.2 Tools and options

In addition to the main interface described above, SAKI offers various tools and options to aid in the simulation and analysis process. A new crystal data file can be created using a template, as shown in Figure 7. Experimental diffraction patterns can be processed for resizing, rotation, and alignment. The precise orientation can be expressed in angles and rational indices of the zone axis. Indices of spots and Kikuchi patterns can be displayed based on intensity thresholds. Conversion between Miller indices and Miller-Bravais indices is also supported. The output area can be configured and saved in .jpg, .png or .tif format. Additionally, SAKI includes a periodic table of elements and a list of space groups to assist in analysis.

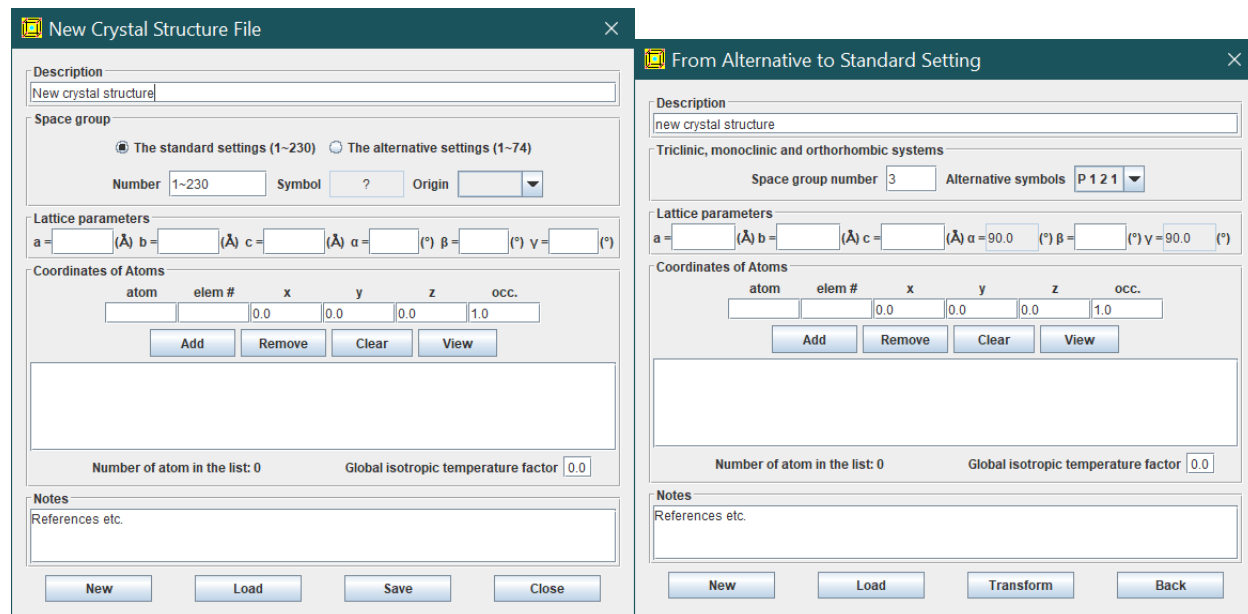


Figure 7. A snapshot of the crystal data templates, standard, and alternative settings.

### 4. Usage of SAKI

SAKI is primarily coded in Java and partially coded for PCs with Microsoft Windows only. Therefore, the Landyne suite requires a Java Runtime Environment, such as openJDK21. SAKI

is a key component of the Landyne software suite, which can be downloaded from the Landyne website:

<https://landyne.com>

To install, decompress the installation file landyne6.z7 in a selected directory and execute landyne.exe by double-clicking. Using SAKI is straightforward: load structure data and set up input parameters, then click the "Simulate" button in the Simulation control panel.

Here are the necessary steps for using SAKI:

1. **Toolbar Functions:** The toolbar displays the most frequently used functions, which can be hidden for small monitors.
2. **Creating Crystal Data:** A new crystal data file can be created using the provided template.
3. **Loading Crystal Data:** A crystal data file can be loaded through the menu file system.
4. **Loading Diffraction Patterns:** Experimental diffraction patterns in JPEG, PNG or TIFF format can be loaded via the menu file system or directly by drag-and-drop.
5. **Determining Precise Orientation:** The precise orientation can be derived using three Kikuchi poles in the experimental diffraction pattern. Two methods are available: analytical equations and vector analysis.
6. **Simulating Patterns:** Click the "Simulate" button in the simulation dialogue panel to create diffraction spots and Kikuchi patterns. Adjust resizing and rotation and choose appearance and other display options.
7. **Indexing Patterns:** Spot patterns and Kikuchi lines can be indexed separately.
8. **Converting Indices:** Miller and Miller-Bravais indices can be converted using the hexagonal system dialogue panel.
9. **Saving Results:** The result can be saved as an image in JPEG, PNG, or TIFF format.

#### *4.1 Prepare new data file*

A structure data file can be prepared using the New Crystal Structure File dialogue window shown in Figure 7. This dialogue window provides an automatic assistant to ensure the file format requirements are met. The template includes the 230 space groups in Hermann-Mauguin notation, as listed in the International Tables for Crystallography. In the monoclinic system, only the unique axis 'b' will be used. Two origin choices can be accepted as input parameters, but choice 2 will be converted to choice 1. To save the data structure, click the "Save" button, or to create a new one, click the "New" button.

The crystal file can also be converted from previous data for modification or from a crystallographic information file (CIF). If a data file in an alternative setting of a space group for triclinic, monoclinic, and orthorhombic systems is used, click on the alternative settings (1~74). A tool is provided for transforming files in non-conventional notations to the standard notations.

#### *4.2 Simulation*



**Orientation and mirror operation** are used to orient the simulated pattern to match the experimental pattern and generate various twins.

**Diffraction patterns** can be viewed in open or solid circles and various colors. A kinematical or double diffraction pattern can be displayed. The index can be labeled for basic reciprocal vectors and diffraction spots selected by the intensity level. Basic vectors and Laue center can be displayed and hidden.

#### 4.3 Save figures for publication

Together with experimental images, these simulated patterns can be saved as publication-ready images. Figure 8 illustrates the tools available for (a) region of interest, (b) indexing, (c) zone axis, and (d) figure labeling. Figure 9 shows a simulated image within a selected region, ready to be saved in .tif, .jpg, .png, or .gif formats.

#### 4.4 Load an experimental image

An experimental diffraction pattern can be loaded through the MS-Windows file system or by a drag-and-drop operation. Figure 10 illustrates the three operations available for images. For alignment, select a point on the image with the mouse pointer; right-clicking will center this point on the screen. The resize and rotation operations will alter the image while keeping the selected point unchanged. A new alignment can be performed on the resized and rotated image.

#### 4.5 Operation steps for analysis

SAKI [Li, 2020a] can be used to determine the index and the zone axis of an experimental diffraction pattern and precise orientation using three Kikuchi poles if it belongs to a known crystal structure. Figure 6 shows the analysis dialogue panel.

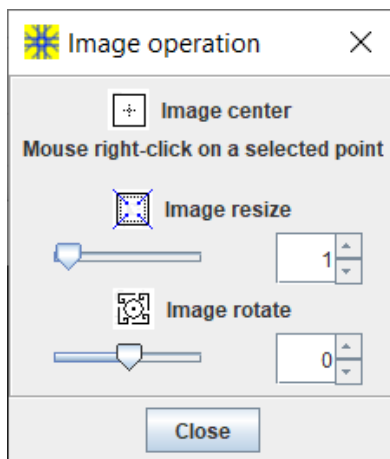


Figure 10. A snapshot of image operation for alignment, resize, and rotation.

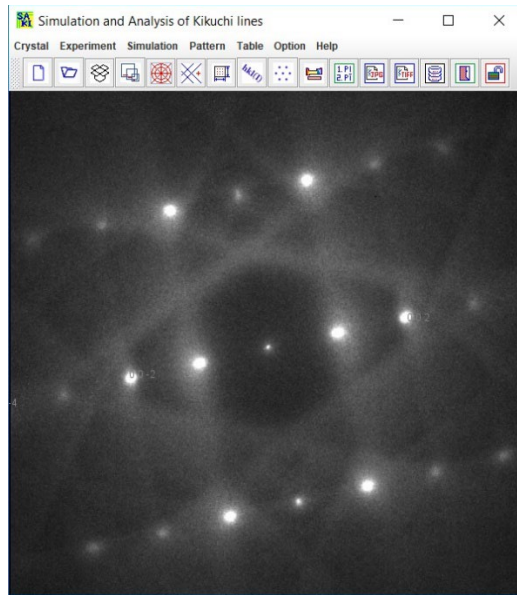


Figure 11. Experimental SAED pattern of the  $\text{Cr}_3\text{Ge}$  phase in the display panel of the SAKI. The zone axis was determined to be  $[210]$ .

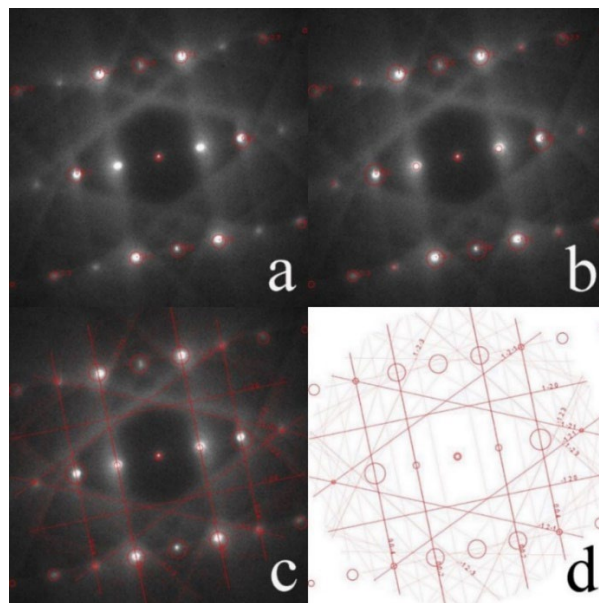


Figure 12. (a) Simulated spot pattern in kinematical diffraction, (b) with a double diffraction effect. (c) Simulated Kikuchi pattern supposed on the experimental pattern (d) the simulated pattern only for clarity.

Steps for analyzing diffraction patterns with SAKI:

1. Set Up R-Spacing Marker:
  - Use the scale bar on the experimental pattern to set up an R-spacing marker.
  - Adjust the calibration circle using the pattern zoom and then lock it down.
2. Select Beam or Kikuchi Pairs:

- In the analysis dialogue panel, choose either the incident beam (default) or one of the Kikuchi pairs (pair1, pair2, pair3).
  - Check the "show" box.
  - Adjust the width, orientation, and position using the mouse.
3. Define Tolerance Values and Search Indices:
    - Define the tolerance value for width (default is 3 pixels) and angle ( $2^\circ$ ).
    - Save the possible indices to a file, then search for the suitable index.
  4. Generate Zone Axes:
    - Generate the zone axes using the input indices of the Kikuchi pairs.
  5. Express Precise Orientation:
    - The precise orientation can be expressed in angles relative to the Kikuchi poles or the zone axis in rational numbers.
    - Convert the Miller-Bravais index for a hexagonal system using the optional tool.
  6. Add Double Diffraction Effects:
    - Add double diffraction effects to SAED diffraction patterns by selecting the appropriate option.

By following these steps, you can accurately analyze and interpret diffraction patterns using SAKI.

## 5. Application examples

Kikuchi analysis has various applications, as listed in the introduction part. Application examples are given in the following.

### 5.1 Simulation of spot and Kikuchi diffraction patterns

The  $\text{Cr}_3\text{Ge}$  phase was found in  $\text{CoFeCrGe}$  Heusler alloy [Jin, Li, Sellmyer 2018]. Figure 11 shows the experimental diffraction pattern of the  $\text{Cr}_3\text{Ge}$  phase. The zone axis was determined to be  $[210]$ . Figure 12 shows (a) a simulated spot pattern in kinematical diffraction, (b) with a double diffraction effect, (c) a simulated Kikuchi pattern supposed on the experimental pattern, and (d) the simulated pattern only for clarity.

Another example of is taken from Figure 2.28(a) on page 23 of Edington's book (1975), which is a complex Kikuchi pattern of the Mg sample. The simulated patterns were carried out separately along all three Kikuchi poles, which shows how the zone axes and Kikuchi line pairs match the experimental pattern, as shown in Figure 13. In the calculation, the high tension of the microscope is assumed to be 100 kV, and the crystal structure of Mg phase, hcp,  $P6_3/mmc$ ,  $a = 3.1094 \text{ \AA}$  and  $c = 5.2108 \text{ \AA}$  is used.

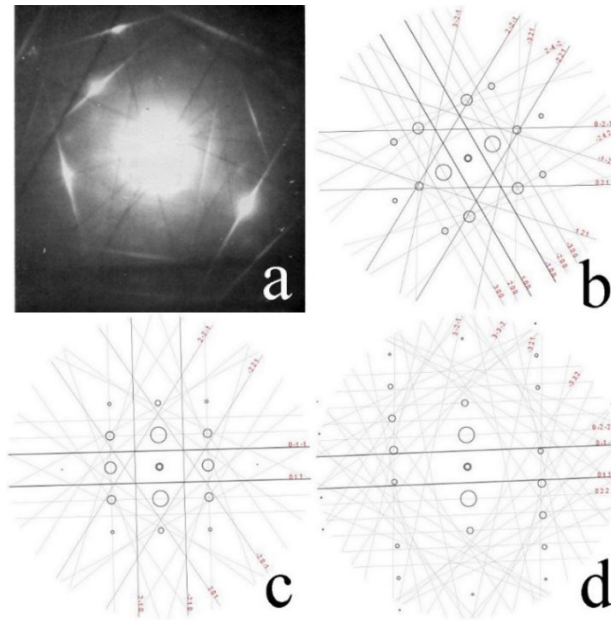


Figure 13. (a) A complex experimental pattern of Mg in Edington’s book. (b-d) Three simulated Kikuchi patterns along the zone axes of  $[0 -1 2]$ ,  $[-1 -2 2]$ , and  $[1 3 -3]$ .

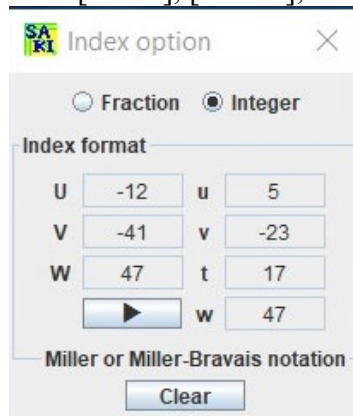


Figure 14. The option for fractional and integer indices and converting Miller indices to Miller-Bravais indices.

### 5.2 Precise orientation determination from three Kikuchi bands

The analysis of the Kikuchi pattern for Mg taken from Edington’s book (1975) is shown in Figure 6 with the parameters and results. The results are listed in Table 2 for a comparison of SAKI. Figure 14 shows the fractional and integer index options and converting Miller indices to Miller-Bravais indices for the hexagonal system. Due to the accuracy in measurement of the Kikuchi pairs in Edington’s book and SAKI, the results are slightly different

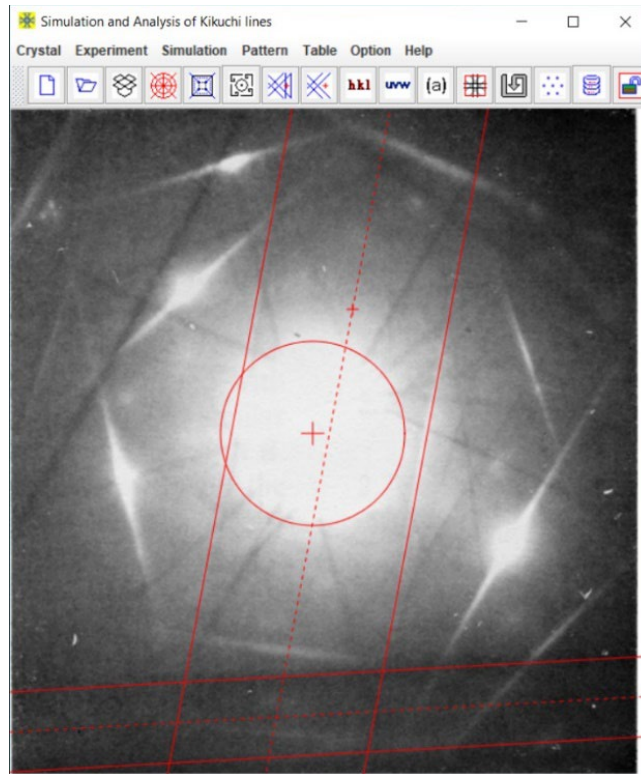


Figure 15. The main panel of SAKI5 features an experimental Kikuchi diffraction pattern. The position of the incident beam has been defined, along with the positions, widths, and directions of two independent pairs of Kikuchi lines.

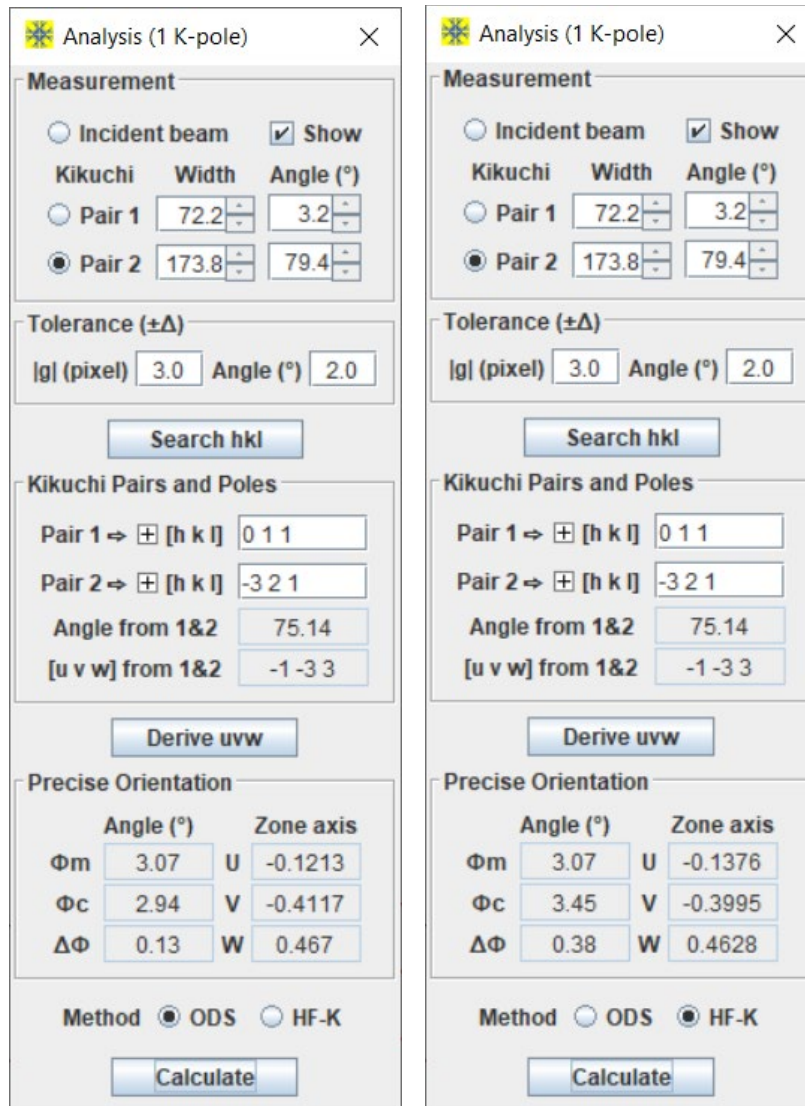


Figure 16. Operational dialog box within SAKI5 for measuring Kikuchi pattern and precisely determining crystal orientation. The applications of (a) the ODS method and (b) the HF-K method.

Table 2. Results from Edington's book and SAKI

Analysis	$\Phi_1$	$\Phi_2$	$\Phi_3$	[u v t w]
Edington's book	3.1°	11.1°	6.5°	[1, -6.024, 5.04, 13.98]
SAKI (measured values)	3.17°	10.37°	6.51°	See the next two rows.
SAKI (analytical method)	3.11°	10.36°	6.48°	[-0.1211, -0.4099, 0.4690]
SAKI (vector method)	3.15°	10.32°	6.57°	[-0.1197, -0.4104, 0.4699]

### 5.3 Precise orientation determination from two Kikuchi bands

The determination of crystal orientation was also done with both the ODS method and the HF-K method. Figure 15 depicts the main graphical interface of the SAKI5, including an experimental diffraction pattern. Figure 16 showcases the analysis dialog box, featuring options for (a) the

ODS method and (b) the HF-K method. The results are displayed in the lower part of the dialog box in Figure 16. The calculated angles are also listed alongside their corresponding measured angles. As shown in Table 3, the results from both methods are consistent with the previous outcomes obtained using three Kikuchi line pairs (or three Kikuchi poles), thereby affirming the practical utility of these two methods.

Due to measurement errors associated with the positions of the incident beam and Kikuchi line pairs in each measurement, there exists a slight angular discrepancy between the incident beam and the Kikuchi pole in both measurements. Comparing the two methods, the angle calculated by the ODS method ( $2.94^\circ$ ) is slightly smaller than the measured angle ( $3.07^\circ$ ). The angle calculated by the HF-K method ( $3.45^\circ$ ) is slightly larger than the measured angle ( $3.07^\circ$ ). However, when averaging the zone axes [UVW] obtained from both methods, the calculated angle ( $3.11^\circ$ ) is very close to the measured angle ( $3.07^\circ$ ), as shown in Table 3.

Table 3. The results of the two methods and the averaged values

Method	U	V	W	$\Phi_c$ ( $^\circ$ )	$\Delta\Phi$ ( $^\circ$ )
ODS	-0.1213	-0.4117	0.467	2.94	0.13
HF-K	-0.1376	-0.3995	0.4628	3.45	0.38
Average	-0.1295	-0.4056	0.4649	3.11	0.04

## 6. Related components in Landyne suite

All software components in the Landyne suite use the input structure data in the same format. A selection of them is listed here, which can be used in combination with the SAKI. Users may check the program specification or user's manual for each program in detail.

### 6.1 SVAT software

SVAT [2020b] is a structural viewer and an analytical tool that uses the same input data format in the Landyne suite and users.

### 6.2 SAED software

SAED [Li, 2019] can simulate spot patterns from multiple crystal files for comparison or for the simulation of various twins and coexisting structures with a fixed orientation. SAKI is used to analyze precise orientation, and SAED is used for the determination of the zone axis. SAKI and SAED can be viewed as an extension of each other.

### 6.3 SPICA software

SPICA [Li, 2016] is designed for stereographic projection with an application for specimen orientation adjustment using TEM holders. SPICA can be used to generate a Kikuchi map.

## References

- Edington, J. W., Practical Electron Microscopy in Materials Science, Monograph Two: Electron Diffraction in the Electron Microscope. Philips, 1975.
- Helfmeier H. and Feller-Kniepmeier M., Analytical Determination of the Exact Primary Beam Direction from Kikuchi Patterns. *J. Appl. Phys.* 48 (1977) 3997.
- Jin, Y.L., Li, X.Z. and Sellmyer, D.J., A new tetragonal phase in CoFeCrGe Heusler alloy, *Mater. Charter.* 136 (2018) 302-309.
- Kuo, K.H., Ye, H.Q. and Wu, Y.K., Application of Electron Diffraction Pattern in Crystallography (in Chinese), Science Press, Beijing, 1983.
- Li. X.Z., SPICA - Stereographic Projection for Interactive Crystallographic Analysis. *J. Appl. Cryst.* 49 (2016) 1818-1826.
- Li. X.Z., On precise determination of crystal orientation with Kikuchi pattern, *Journal of Materials Education*, 42:1-2 (2020a) 97-104.
- Li. X.Z., SVAT4 – a computer program for crystal structure visualization and analysis *J. Appl. Cryst.* 53(2020b) 848-853.
- Li. X.Z., SAED3: simulation and analysis of electron diffraction patterns. *Microscopy and Analysis*, May issue (2019) 16-19.
- Liu, W.X., Huang, X.Y. and Chen, Y.R., Electron Microscopy Analysis on Material Structures (in Chinese), Tianjin University press, 1989.
- Otte, H.M., Dash, J. and Schaak, H.F., Electron Microscopy and Diffraction of Thin Films : Interpretation and Correlation of Images and Diffraction Patterns. *Phys. Stat. Sol.* 5 (1964) 527-549.
- Thomas, G. and Goringe, M.J., Transmission Electron Microscopy of Materials, John Wiley & Sons, 1979.